Dramatic volcanic instability revealed by InSAR

L.N. Schaefer[1], Z. Lu[2], and T. Oommen[1]
[1]Department of Geological and Mining Engineering and Sciences, Michigan Technological University, Houghton, Michigan 49931, USA
[2]Roy M. Huffington Department of Earth Sciences, Southern Methodist University, Dallas, Texas 75275, USA

ABSTRACT

Interferometric synthetic aperture radar (InSAR) was used to measure ground deformation during explosive eruptions on 27 and 28 May 2010 at Pacaya volcano, Guatemala. Interferograms produced using spaceborne and airborne synthetic aperture radar data reveal ~3 m of along-slope movement of the southwest sector of the edifice during these eruptions. This is the largest measured slope instability witnessed in a single event at a volcano that did not result in a catastrophic landslide. This rapid and extreme movement is particularly concerning given the history of sector collapse and persistent activity at this volcano. These findings emphasize the utility of high-resolution InSAR measurements for monitoring deformation and potential catastrophic slope instability at volcanoes.

INTRODUCTION

The structural failure of volcanoes has been widely recognized as a pervasive and potentially devastating phenomenon, given the historic volcanic sector collapses of Bezymianny (Kamchatka, Russia, 1956), Sheveluch (Kamchatka, Russia, 1964), and Mount St. Helens (Washington, USA, 1980) (see Carrasco-Núñez et al., 2011, and references therein). One way to identify regions of instability on volcanoes is to monitor deformation using geodetic techniques. Currently, deformation has been measured at 214 volcanoes (Volcano Deformation Database; globalvolcanomodel.org/gvm-task-forces/volcano-deformation-database/), 160 of which were measured using interferometric synthetic aperture radar (InSAR). InSAR, in which the phase of 2 or more synthetic aperture radar images are differenced to determine surface deformation, has been used to study more than 500 volcanoes worldwide since the 1990s (Biggs et al., 2014) and has high accuracy (<1 cm) over large areas (several cubic kilometers or more).

Here we use interferometric data from the Advanced Land Observing Satellite (ALOS; L-band, λ = 23 cm) to measure ground deformation during explosive and effusive eruptions on 27 and 28 May 2010 at Pacaya volcano, Guatemala. This was compared to Uninhabited Aerial Vehicle Synthetic Aperture Radar (UAVSAR; L-band) aircraft and GPS data. Several possibilities for the origin of deformation of the southwest flank are considered against interferometric results and existing structural and volcanological information.

BACKGROUND

Pacaya is a basaltic to dacitic stratovolcano complex in Guatemala, located on the southern rim of the Amatitlán caldera 25 km south of the capital, Guatemala City (Fig. 1A). During an explosive phase between 3000 and 700 yr ago, the southwest sector of the cone failed in a major collapse, forming a debris avalanche that traveled 25 km southwest (Fig. 1B), with an estimated volume of 0.65–0.8 km³ (Vallance et al., 1995). Dating of two tephra fall deposits by Kitamura and Matías (1995) confine the age of the sector collapse within 1500–600 yr ago. Episodic activity since the 16th century rebuilt the edifice within the collapse amphitheater, creating the Cerro Chino and modern Pacaya cone. However, the scarp from the collapse is still visible on the north and northeast sides of the volcano (Figs. 1B and 1C). After a period of repose beginning in the mid-19th century, activity renewed once again in 1961 with a flank eruption that continued for one month (Eggers, 1971). In June of 1962, an ~300 × 200 m oval-shaped area subsided near the summit (Fig. 1C), and was quickly filled by erupted material during the following years (Eggers, 1971). Since 1961, eruptive activity has been very frequent, with extended periods of constant lava effusion and small explosive activity (e.g., from 2004 to 2010), producing more than 250 lava flows, intermittent Strombolian activity, and ash and gas plumes (Matías Gómez et al., 2012).

Details of the May 2010 Eruptions

This study focuses on eruptive events in May 2010; details are derived from reports by Guatemala's National Institute of Seismology, Volcanology, Meteorology, and Hydrology (www.insivumeh.gob.gt), the National Coordinator for Disaster Reduction (www.conred.gob.gt), and the Global Volcanism Program (www.volcano.si.edu). On the evening of 27 May, intense lava fountaining and vigorous ejection of tephra and ballistics erupted from the summit vent. Seismicity records show an increase in real-time seismic amplitude measurement (RSAM) values during the afternoon of the same day, peaking shortly before 1800 h local time and lasting
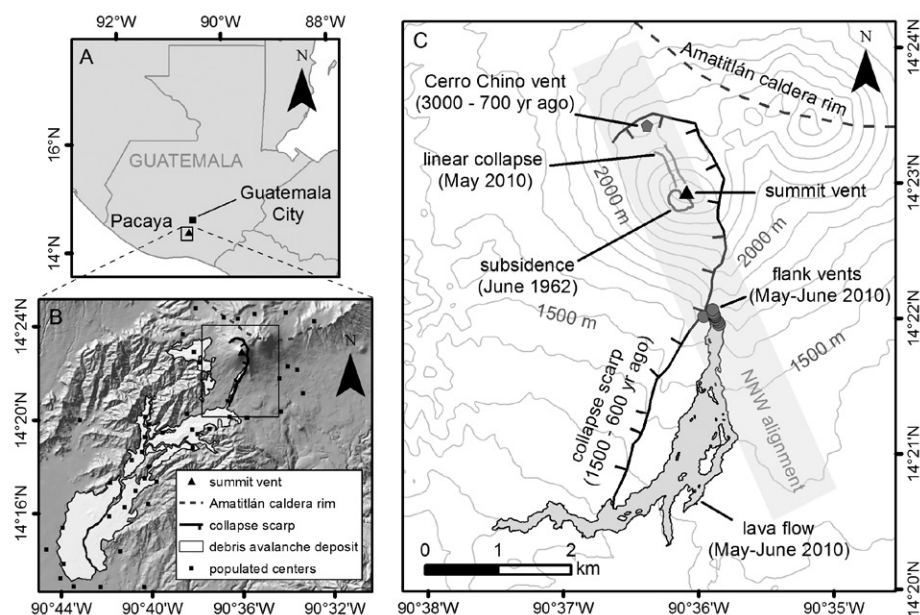

Figure 1. A: Location of Pacaya volcano, Guatemala, 25 km south of Guatemala City. B: Map showing locations of current populated centers and the extent of the debris avalanche deposit (modified from Kitamura and Matías, 1995) from the sector collapse dated between and 1500 and 600 yr ago and the resulting collapse scarp. Outline shows area of C and Figure 2. C: Structural map with additional features including the Cerro Chino vent, the June 1962 subsidence, the May 2010 linear collapse, and the flank vents and deposition of the May–June 2010 lava flow that erupted outside of the collapse scarp. These features are aligned in a north-northwest pattern orthogonal to the direction of flank movement.
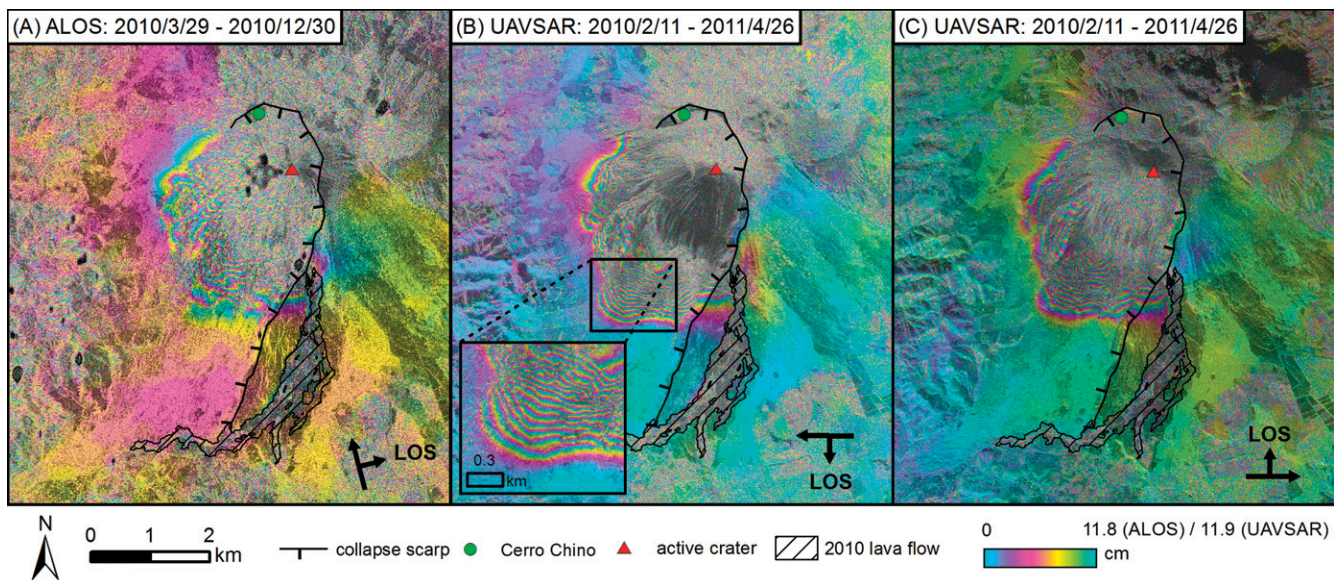
Figure 2. Radar interferometry results spanning the 27–28 May eruptions of Pacaya volcano, Guatemala. Combining the different look angles of the Uninhabited Aerial Vehicle Synthetic Aperture Radar (UAVSAR) and Advanced Land Observing Satellite (ALOS) interferograms allows us to interpret the Interferometric synthetic aperture radar (InSAR) phases as ~3 m of along-slope movement of the southwest flank. LOS—line of sight. Location outlined in Figure 1B. A: ALOS. Each fringe (full color cycle) represents 11.8 cm of range change between the ground and the satellite. B, C: UAVSAR. Each fringe (full color cycle) represents 11.9 cm of range change between the ground and the satellite. Zoomed view in B shows details of close spacing and irregular contact of the fringe pattern.

~40 min (see Fig. DR1 in the GSA Data Repository[1]). The ejected material destroyed or damaged nearly 800 homes and forced more than 2500 residents in nearby communities to evacuate. A collapse feature 50–80 m deep and 100 m wide, extending 600 m from the summit, developed concurrent with explosive activity from the summit vent (Fig. 1C). Southerly winds dispersed tephra over Guatemala City, covering an area of >1000 km[2]. This tephra and ash blanket was estimated to be 20 cm thick directly north of Pacaya and 0.5–10 cm thick in Guatemala City (Matías Gómez et al., 2012; Fig. DR2). Violent Strombolian eruptions resumed on 28 May, with seismicity records again showing a peak in RSAM values shortly before 1100 h local time, lasting slightly longer than 1 h. On this day, a lava flow erupted from 12 clustered flank vents outside of the collapse scarp to the southeast of the summit ~1700 m above sea level (asl) (Fig. 1C). This lava flow reached >5 km in length, and had an estimated volume of $1.74–6.96 \times 10^6$ m[3] (Matías Gómez et al., 2012). Summit activity decreased significantly on 29 May, with only small eruptive plumes and minor tephra fall, and continued to decrease in the following days. An estimated tephra volume of 1.3×10^7

m[3] (see Matías Gómez et al., 2012, and references therein) ranks the 27–28 May eruptions as a VEI-3 (volcano explosivity index). However, this does not take into account the large volume of lava erupted from the flank vent, which nearly doubles the eruptive products.

The 1962 subsidence and the 2010 linear collapse, combined with the ancestral sector collapse, suggest inherent instability of the edifice. In addition, a possible basement layer of pyroclastics beneath the edifice erupted from the Amatitlán caldera (Eggers, 1971; Wunderman and Rose, 1984; Schaefer et al., 2013), a sloping basement substrate (Vallance et al., 1995), diverse lithologies (Schaefer et al., 2015), and uneven loading of lava flows on the southwest flank (Matías Gómez et al., 2012) have all been cited as causes of concern for the stability of this young edifice.

InSAR DATA

ALOS interferograms that span the 27–28 May eruptions contain dense fringes that form a semicircle from the Cerro Chino cone to the flank vents outside of the collapse scarp (Fig. 2A). The observed fringes are not caused by topography-related errors, as other interferograms with larger baselines do not exhibit similar fringe patterns (Fig. DR3). InSAR signal correlation, termed coherence, breaks down at elevations above 1500 asl on the southwest flank and 1700 asl on the west flank (pixilated regions in Figs. 2A–2C). This could be due to high deformation rates above InSAR detection limits within one 7.5 m pixel (11.8 cm in the case of ALOS), or changes of scattering proper-

ties within pixels due to thick (~20 cm) tephra deposition during the eruption. The area to the north of the cone is also incoherent due to this tephra deposition. Good coherence to the east, west, and south of the cone reflect the fact that tephra and other eruptive material were not deposited in these regions. Phase unwrapping, where the correct integer multiple of 2π is added to the interferometric fringes to produce a continuous deformation field, was discarded due to phase jumps and errors in low coherence and high deformation-gradient areas.

ALOS results were compared to UAVSAR interferograms, processed by the NASA Jet Propulsion Laboratory (JPL), but cropped to Pacaya's extent and filtered for this study. The UAVSAR interferograms produced from two independent acquisitions on both 11 February 2010 and 26 April 2011 show fringe patterns similar to the ALOS interferogram. In addition, UAVSAR interferograms allow us to clarify deformation that is not resolvable in regions of the ALOS interferograms because of higher resolution (~2 m pixel size) and negligible changes in instrument viewing geometry (i.e., zero baseline) (Figs. 2B and 2C). The two UAVSAR interferograms were acquired on the same dates but with opposite looking geometry, west-bound south looking (Fig. 2B) versus east-bound north looking (Fig. 2C). Combining the two UAVSAR interferograms with the ALOS interferogram, we interpret the InSAR phases as west to southwestward and downslope motion of the southwest sector of the cone.

Based on terrain geometry and SAR instrument imaging (see Zhao et al., 2012), along-

slope displacement can be calculated from the line of sight (LOS) displacement. Thus, the ~60 cm of deformation in the ALOS interferogram corresponds to ~300 cm of westward and downslope motion. For the UAVSAR interferograms, the LOS displacement of ~190 cm suggests ~270 cm of westward and downslope motion. Therefore, the amount of motion inferred from the three independent interferograms is about the same.

Comparison of InSAR Results with GPS Measurements

The direction of movement observed with InSAR is supported by GPS measurements made by Michigan Technological University (Houghton, Michigan) and Hetland (2014). From January 2009 to March 2013, a station on the southwest flank (see Fig. DR4 for GPS location map and measured velocities) measured 0.22 m of movement to the southwest and –0.5 m of vertical movement, resulting in a total (three-dimensional) displacement of 0.54 m to the southwest. In the same study, GPS measurements did not detect this movement prior to (October 2001 to January 2009) and after (January 2011 to March 2013) the eruption period. Measurements made from a station near the Cerro Chino cone show that similar downward and southwestward movement occurred at the summit. This suggests that the upper flanks of the edifice also deformed, a measurement point that is lost in the InSAR results due to incoherence from eruptive products. The difference in the magnitude of flank movement calculated from GPS and InSAR could be due to several possible errors reported by Hetland (2014), including coarse temporal sampling of the GPS network (1–2 times per year from January 2009 to September 2011 and 3–4 times per year from September 2011 to March 2013), short acquisition periods during sampling, or false displacement signatures due to station damage. However, the direction of flank movement, interpreted to be volcanic edifice slip (Hetland, 2014), is similar to what we measure with InSAR.

DISCUSSION

A range of processes can cause a volcanic edifice to deform, including gravitationally driven creep, heavy rainfall, destabilization due to earthquakes, magmatic processes, and settling and compaction of the edifice. At Pacaya, the opposite-looking UAVSAR interferograms suggest that the motions are mostly horizontal, as the fringe patterns are nearly symmetric and the sense of motion is opposite in the two images (Figs. 2B and 2C). That is, the fringes are not indicative of edifice inflation or deflation due to changes in a pressurized magma chamber, which would contain more vertical components. This is also supported by the lack of deformation signal in the coherent areas of the southeastern and eastern flanks, which would probably deform in such an event (e.g., roughly axisymmetric deformation; Pritchard and Simons, 2002). Instead, the high frequency and close spacing of the fringes, which have irregular contact and end abruptly at the toe of the slope, are indicative of landsliding motion.

The mechanics of the sliding movement are difficult to resolve because of incoherence at the summit. Previous numerical modeling at Pacaya (Schaefer et al., 2013) has shown that for deformation to reach the flank's lower elevations where the InSAR fringes are located, the unstable mass is likely to have a profile reminiscent of other large volcanic sector collapses (see Siebert, 1984; Fig. DR6), as opposed to shallow sliding of only surface material (i.e., Ebmeier et al., 2014). In addition, the involvement of a large amount of material and the direction of movement match well with the volcano's previous sector collapse. At other volcanoes, gravitationally driven creep has been inferred as the primary deformation mechanism (e.g., Borgia and van Wyk de Vries, 2003). This can be ruled out at Pacaya, as a separate interferometric survey detected no deformation of the edifice between 2007 and 2010 (Ebmeier et al., 2013); we confirm this with ALOS data (Fig. DR5).

ALOS interferograms processed from SAR images acquired before and after the event do not show the high-frequency deformation fringe pattern seen in interferograms that span the May eruptions (Fig. DR5), allowing us to confine the deformation between 29 March and 31 May 2010. As the flank moved to the southwest, this movement could have caused the linear collapse trending orthogonally to the motion as a result of tensional failure, as typically seen in spreading structures (Merle and Borgia, 1996). Because eye witnesses observed the formation of the trough during the May eruptions, we can link the slope movement with the trough formation. Coeruptive deformation is further supported by seismic records; other than the RSAM peaks on the 27 and 28 May that correspond with eruptions, there is no seismic evidence of edifice movement (Fig. DR1). This suggests that flank movement occurred during one or both of the eruption peaks, and any seismic signal associated with the motion was overwhelmed during explosive activity. No large tectonic earthquakes were recorded during this timeframe, allowing us to discount tectonic movement as a trigger. This time restraint also allows us to rule out flank instability due to rainfall associated with tropical storm Agatha, which made landfall in Guatemala on the evening of 29 May.

The alignment of the Cerro Chino cone, summit, 2010 linear collapse, and flank vents trending north-northwest (Fig. 1C) suggest a structurally weak zone that controls magma intrusion orientation (Schaefer et al., 2013). This is similar to surface magma plumbing system geometries at other volcanoes with previous sector collapses (e.g., Stromboli; Corazzato et al., 2008). Thus it is possible that strong lateral displacements caused by magma upwelling or volatile intrusion into the edifice along this structurally weak zone both triggered the observed flank movement and created the linear collapse (i.e., Piton de la Fournaise, Sigmundsson et al., 1999; Etna, Billi et al., 2003).

HAZARD IMPLICATIONS

Large-scale edifice collapses have been documented at more than 400 Quaternary volcanoes worldwide (Siebert et al., 2006). Although not as common as other volcanic phenomena, these events are extremely dangerous, producing large volumes (several cubic kilometers or larger) of material that can travel in excess of 50 km and deposit debris over areas of hundreds to thousands of square kilometers (see Carrasco-Núñez et al., 2011, and references therein). Pacaya is surrounded by several communities totaling ~10,000 people that live within 5 km of the active cone (Fig. 1B). The risk of the proximity of these communities to the volcano is clear by the recurrent evacuations during recent eruptions (13 evacuations since 1987; Witham, 2005). One notable feature on both interferograms is that the deformation fringes extend over the collapse scarp (Figs. 2A and 2B), suggesting that the unstable material is not contained within the collapse amphitheater. This also implies that if a sector collapse were to occur in the future, the resulting debris flow could contain a larger portion of the edifice than the last major collapse. Based on national census data from 2002 and population growth estimates from the World Bank (http://data.worldbank.org/data-catalog/population-projection-tables), a debris avalanche with a volume and direction similar to the previous collapse could affect more than 11,000 people (Fig. DR7). Evidence of a magma reservoir high in the cone (Eggers, 1983) suggests that a collapse event could cause rapid decompression of shallow magma, potentially affecting areas outside of the debris avalanche deposit zone. This was further evidenced by Kitamura and Matías (1995), who mapped blast deposits from the previous Pacaya sector collapse several kilometers outside of the debris avalanche deposits to the north and west of the cone. The rapid movement concurrent with explosive activity measured in this study, without any prior or sequential movement, emphasizes the need for higher data temporal resolution to mitigate risk.

CONCLUSIONS

Interferograms processed from the ALOS satellite and compared against aerial UAVSAR and GPS data were used to investigate volcanic deformation associated with the 27–28 May 2010 eruptions of Pacaya volcano in Guatemala.

InSAR techniques have allowed us to measure ~3 m of movement of the lower southwest flank where the interferometric signal remained coherent. The close, irregular fringe spacing and abrupt termination of fringes indicate along-flank slope displacement. The good spatial coverage of the InSAR data has allowed us to measure this large slope movement that would have been undetected with GPS, seismic, or field observations alone, highlighting the utility of these methods for monitoring volcanic deformation and potential catastrophic slope instability. Remote monitoring is particularly useful at Pacaya, where nearly constant effusive and explosive activity makes it difficult to use ground monitoring techniques. The markedly improved quality of the UAVSAR interferogram shows that there are several advantages to using zero-baseline and higher pixel resolution SAR for resolving deformation details. In addition, the uniqueness of this flank movement emphasizes the importance of differing SAR instrument look angles for resolving movement components. The rapid and widespread movement concurrent with explosive activity emphasizes the need for data with broad spatial coverage and high temporal resolution at other potentially unstable volcanoes. We conclude that the deformation measured at Pacaya volcano indicates that slope failure is a serious threat, and that monitoring deformation, particularly during eruptive events, is crucial for hazard purposes.

REFERENCES CITED
Biggs, J., Ebmeier, S.K., Aspinall, W.P., Lu, Z., Pritchard, M.E., Sparks, R.S.J., and Mather, T.A., 2014, Global link between deformation and volcanic eruption quantified by satellite imagery: Nature Communications, v. 5, 3471, doi: 10.1038/ncomms4471.

Billi, A., Acocella, V., Funiciello, R., Giordano, G., Lanzafame, G., and Neri, M., 2003, Mechanisms for ground-surface fracturing and incipient slope failure associated with the 2001 eruption of Mt. Etna, Italy: Analysis of ephemeral field data: Journal of Volcanology and Geothermal Research, v. 122, p. 281–294, doi:10.1016/S0377-0273(02)00507-3.

Borgia, A., and van Wyk de Vries, B., 2003, The volcano-tectonic evolution of Concepción, Nicaragua: Bulletin of Volcanology, v. 65, p. 248–266, doi:10.1007/s00445-002-0256-8.

Carrasco-Núñez, G., Siebert, L., and Capra, L., 2011, Hazards from volcanic avalanches, in Veress, B., and Szigethy, J., eds., Horizons in Earth Science Research Volume 3: New York, Nova Science Publishers, Inc., p. 199–227.

Corazzato, C., Francalanci, L., Menna, M., Petrone, C., Renzulli, A., Tibaldi, A., and Vezzoli, L., 2008, What controls sheet intrusion in volcanoes? Petrological and structural characters of the Stromboli sheet complex, Italy: Journal of Volcanology and Geothermal Research, v. 173, p. 26–54, doi:10.1016/j.jvolgeores.2008.01.006.

Ebmeier, S.K., Biggs, J., Mather, T.A., and Amelung, F., 2013, On the lack of InSAR observations of magmatic deformation at Central American volcanoes: Journal of Geophysical Research, v. 118, p. 2571–2585, doi:10.1002/jgrb.50195.

Ebmeier, S.K., Biggs, J., Muller, C., and Avard, G., 2014, Thin-skinned mass-wasting responsible for deformation at Arenal volcano: Frontiers in Earth Science, v. 2, doi:10.3389/feart.2014.00035.

Eggers, A., 1971, The geology and petrology of the Amatitlán Quadrangle, Guatemala [Ph.D. thesis]: Hanover, New Hampshire, Dartmouth College, 235 p.

Eggers, A.A., 1983, Temporal gravity and elevation changes at Pacaya volcano, Guatemala: Journal of Volcanology and Geothermal Research, v. 19, p. 223–237, doi:10.1016/0377-0273(83)90111-7.

Hetland, B.R., 2014, A surface displacement analysis for Volcan Pacaya from October 2001 through March 2013 by means of 3-D modeling of precise position GPS data [M.S. thesis]: Houghton, Michigan, Michigan Technological University, 84 p.

Kitamura, S., and Matías, O., 1995, Tephra stratigraphic approach to the eruptive history of Pacaya volcano, Guatemala:–Tohoku University Science Reports, Seventh Series, v. 45, p. 1–41.

Matías Gómez, R.O., Rose, W.I., Palma, J.L., and Escobar-Wolf, R., 2012, Notes on a map of the 1961–2010 eruptions of Volcán de Pacaya, Guatemala: Geological Society of America Digital Map Chart Series 10, 10 p., doi:10.1130/2012.DMCH010.

Merle, O., and Borgia, A., 1996, Scaled experiments of volcanic spreading: Journal of Geophysical Research, v. 101, p. 13,805–13,817, doi:10.1029/95JB03736.

Pritchard, M.E., and Simons, M., 2002, A satellite geodetic survey of large-scale deformation of volcanic centres in the central Andes: Nature, v. 418, p. 167–171, doi:10.1038/nature00872.

Schaefer, L.N., Oommen, T., Corazzato, C., Tibaldi, A., Escobar-Wolf, R., and Rose, W.I., 2013, An integrated field-numerical approach to assess slope stability hazards at volcanoes: The example of Pacaya, Guatemala: Bulletin of Volcanology, v. 75, doi:10.1007/s00445-013-0720-7.

Schaefer, L.N., Kendrick, J.E., Lavallée, Y., Oommen, T., and Chigna, G., 2015, Geomechanical rock properties of a basaltic volcano: Frontiers in Earth Science, v. 3, 29 p., doi:10.3389/feart.2015.00029.

Siebert, L., 1984, Large volcanic debris avalanches: Characteristics of source areas, deposits, and associated eruptions: Journal of Volcanology and Geothermal Research, v. 22, p. 163–197, doi:10.1016/0377-0273(84)90002-7.

Siebert, L., Alvarado, G.E., Vallance, J.W., and van Wyk De Vries, B., 2006, Large-volume volcanic edifice failures in Central America and associated hazards, in Rose, W.I., et al., eds., Volcanic hazards in Central America: Geological Society of America Special Paper 412, p. 1–26, doi:10.1130/2006.2412(01).

Sigmundsson, F., Durand, P., and Massonnet, D., 1999, Opening of an eruptive fissure and seaward displacement at Piton de la Fournaise volcano measured by RADARSAT satellite radar interferometry: Geophysical Research Letters, v. 26, p. 533–536, doi:10.1029/1999GL900055.

Vallance, J.W., Siebert, L., Rose, W.I., Raul Girón, J., and Banks, N.G., 1995, Edifice collapse and related hazards in Guatemala: Journal of Volcanology and Geothermal Research, v. 66, p. 337–355, doi:10.1016/0377-0273(94)00076-S.

Witham, C.S., 2005, Volcanic disasters and incidents: A new database: Journal of Volcanology and Geothermal Research, v. 148, p. 191–233, doi:10.1016/j.jvolgeores.2005.04.017.

Wunderman, R.L., and Rose, W.I., 1984, Amatitlán, an actively resurging cauldron 10 km south of Guatemala City: Journal of Geophysical Research, v. 89, p. 8525–8539, doi:10.1029/JB089iB10p08525.

Zhao, C., Lu, Z., Zhang, Q., and de La Fuente, J., 2012, Large-area landslide detection and monitoring with ALOS/PALSAR imagery data over northern California and southern Oregon, USA: Remote Sensing of Environment, v. 124, p. 348–359, doi:10.1016/j.rse.2012.05.025.